Light-induced phase and amplitude gratings in centrosymmetric Gadolinium Gallium garnet doped with Calcium

Mostafa A. Ellabban[1], **Martin Fally, Romano A. Rupp**

Fakultät für Physik, Universität Wien, Boltzmanngasse 5, A-1090 Wien, Austria
[1]*on leave from: Faculty of Science, Tanta University, Egypt*

László Kovács

Crystal Physics Laboratory, Research Institute for Solid State Physics and Optics, Hungarian Academy of Sciences, H-1525 Budapest, P.O. Box 49, Hungary

Martin.Fally@univie.ac.at

http://nlp.exp.univie.ac.at

Abstract: The photosensitive properties of a centrosymmetric gadolinium gallium garnet crystal doped with calcium are investigated at room temperature. Elementary holograms can be recorded over a wide range of wavelengths in the visible spectral range. The photosensitive properties are studied experimentally using beam coupling and angular response experiments. Mixed absorption and refractive-index gratings are observed and their amplitudes and relative phases determined. Moreover, the candidate centers that are responsible for the photorefractive effect are discussed.

OCIS codes: (090.0090) Holography; (090.7330) Volume holographic gratings; (090.2900) Holographic recording materials.

References and links

1. L. Antos, M. Pardavi-Horvath, A. Cziraki, J. Fidler, and P. Skalicky, "Microstructure of Yttrium Iron Garnet Thin Films and of Gadolinium Gallium Garnet Single Crystals," J. Cryst. Growth **94**, 197–02 (1989).
2. A. S. Yurov, A. N. Karpov, V. K. Raev, G. E. Khodenkov, and M. P. Shorygin, "Displacement of a magnetic bubble by a Rayleigh surface wave in an iron garnet film containing bismuth," Tech. Phys. Lett. **12**, 83–4 (1986).
3. R. Wolfe, "Thin films for non-reciprocal magneto-optic devices," Thin Solid Films **216**, 184–8 (1992).
4. C. S. Tsai, "Wideband tunable microwave devices using ferromagnetic film-gallium arsenide material structures," J. Magn. Magn. Mater. **209**, 10–14 (2000).
5. S. Yamamoto and T. Makimoto, "Design considerations for nonreciprocal integrated optical devices," J. Appl. Phys. **47**, 4056–60 (1976).
6. E. Zharikov, N. Il'ichev, V. Laptev, A. Malyutin, V. Ostroumov, P. Pashinin, and I. Shcherbakov, "Sensitization of neodymium ion luminescence by chromium ions in a $Gd_3Ga_5O_{12}$ crystal," Sov. J. Quantum Electron. **12**, 338–41 (1982).
7. J. Marion, "Strengthened solid-state laser materials," Appl. Phys. Lett. **47**, 694–6 (1985).
8. A. A. Danilov, E. Y. Nikirui, V. V. Osiko, V. G. Polushkin, S. N. Sorokin, and M. I. Timoshechkin, "Efficient laser with a rectangular active element," Sov. J. Quantum Electron. **21**, 264–6 (1991).
9. H. Brusset, H. Giller-Prandraud, and J. L. Bordot, "Investigations on Gallates of Rare Earth Metals and of Yttrium," B. Soc. Chim. Fr. **4**, 1206 (1967).
10. J. Dong and K. Lu, "Noncubic symmetry in garnet structures studied using extended x-ray-absorption fine-structure spectra," Phys. Rev. B **43**, 8808 (1991).
11. G. J. Pogatshnik, L. S. Cain, Y. Chen, and B. D. Evans, "Optical Properties of Color Centers in Calcium-Stabilized Gadolinium Gallium Garnets," Phys. Rev. B **43**, 1787–94 (1991).

#8649 - $15.00 USD Received 1 September 2005; revised 9 January 2006; accepted 14 January 2006

12. R. Metselaar, J. P. M. Damen, P. K. Larsen, and M. A. H. Huyberts, "Investigation of Colour Centres in Gadolinium Gallium Garnet Crystals," Phys. Status Solidi (a) **34**, 665–70 (1976).
13. A. O. Matkovskii, D. Y. Sugak, S. B. Ubizskii, U. A. Ulmanis, and A. P. Shakhov, "Radiation-Stimulated Processes in Gadolinium Gallium Garnet Single Crystals," Phys. Status Solidi (a) **128**, 21–29 (1991).
14. A. Matkovskii, P. Potera, D. Sugak, L. Grigorjeva, D. Millers, V. Pankratov, and A. Suchocki, "Stable and transient color centers in $Gd_3Ga_5O_{12}$ crystals," Cryst. Res. Technol. **39**, 788–795 (2004).
15. G. C. Valley and J. F. Lam, *Theory of Photorefractive Effects in Electro-Optic Crystals*, vol. 61 of *Topics in Applied Physics*, chap. 3, pp. 75–98 (Springer-Verlag, Berlin, 1988).
16. R. Hofmeister, A. Yariv, S. Yagi, and A. Agranat, "New Photorefractive Mechanism in Centrosymmetric Crystals: A Strain-Coordinated Jahn-Teller Relaxation," Phys. Rev. Lett. **69**, 1459–62 (1992).
17. B. Sugg, H. Nürge, B. Faust, E. Ruza, R. Niehüser, H. J. Reyher, R. A. Rupp, and L. Ackermann, "The Photorefractive Effect in Terbium Gallium Garnet," Opt. Mat. **4**, 343–7 (1995).
18. I. Redmond, R. Linke, E. Chuang, and D. Psaltis, "Holographic Data Storage in a DX-Center Material," Opt. Lett. **22**, 1189–91 (1997).
19. M. Imlau, S. Haussühl, T. Woike, R. Schieder, V. Angelov, R. A. Rupp, and K. Schwarz, "Holographic Recording by Excitation of Metastable Electronic States in $Na_2[Fe(CN)_5NO]\cdot 2H_2O$: a new photorefractive effect," Appl. Phys. B **68**, 877–85 (1999).
20. B. Crosignani, A. Degasperis, E. DelRe, P. Di-Porto, and A. J. Agranat, "Nonlinear Optical Diffraction Effects and Solitons Due to Anisotropic Charge-Diffusion-Based Self-Interaction," Phys. Rev. Lett. **82**, 1664–7 (1999).
21. A. E. Krumins, R. A. Rupp, and J. A. Seglins, "Hologram Recording in PLZT Ceramics in the Vicinity of its Diffused Phase Transition," Ferroelectrics **107**, 53–8 (1990).
22. R. MacDonald, R. Linke, J. Chadi, T. Thio, G. Devlin, and P. Becla, "Thick Plasma Gratings Using a Local Photorefractive Effect in CdZnTe:In," Opt. Lett. **19**, 2131–3 (1994).
23. M. Imlau, T. Woike, R. Schieder, and R. A. Rupp, "Holographic Scattering in Centrosymmetric $Na_2[Fe(CN)_5NO]\cdot 2H_2O$," Phys. Rev. Lett. **82**, 2860–3 (1999).
24. M. Pardavi-Horvath, J. Paitz, I. Földvari, I. Fellegvari, and L. Gosztonyi, "Spectroscopic Properties of Ca^{2+} - doped GGG," Phys. Status Solidi (a) **84**, 540–2 (1984).
25. M. Fally, M. Imlau, R. A. Rupp, M. A. Ellabban, and T. Woike, "Specific recording kinetics as a general property of unconventional photorefractive media," Phys. Rev. Lett. **93**(24), 243,903 (2004).
26. D. L. Wood and K. Nassau, "Optical Properties of Gadolinium Gallium Garnet," Appl. Opt. **29**, 3704–7 (1990).
27. M. Pardavi-Horvath and M. Osvay, "Thermoluminescent Properties of Gadolinium Gallium Garnet Crystals Containing Ca^{2+} Impurity," Phys. Status Solidi (a) **80**, K183–5 (1983).
28. A. Matkovskii, D. Sugak, S. Ubizskii, and I. Kityk, "Spectroscopy and radiation defects of the $Gd_3Ga_5O_{12}$ single crystals," Opto-Electron. Rev. **3**, 41–53 (1995).
29. E. Guibelalde, "Coupled wave analysis for out-of-phase mixed thick hologram gratings," Opt. Quantum Electron. **16**, 173 (1984).
30. V. L. Vinetskiĭ, N. V. Kukhtarev, S. G. Odulov, and M. S. Soskin, "Dynamic self-diffraction of coherent light beams," Sov. Phys. Usp. **22**, 742–756 (1979).
31. F. Kahmann, "Separate and Simultaneous Investigation of Absorption Gratings and Refractive-Index Gratings by Beam-Coupling Analysis," J. Opt. Soc. Am. A **10**, 1562–9 (1993).
32. C. Neipp, I. Pascual, and A. Beléndez, "Experimental evidence of mixed gratings with a phase difference between the phase and amplitude grating in volume holograms," Opt. Express **10**, 1374–83 (2002), http://www.opticsexpress.org/abstract.cfm?URI=OPEX-10-23-1374.

1. Introduction

Gadolinium gallium garnet ($Gd_3Ga_5O_{12}$, GGG) belongs to the most perfect materials that are grown in large quantities with a dislocation density of less than $3/cm^3$ [1]. Owing to that it is one of the most appropriate substrate materials for magnetic bubble memory [2], magneto-optic [3], integrated optical and microwave devices [4, 5]. Moreover, GGG is applied as a host material in highly efficient solid-state lasers [6, 7, 8].

GGG has the molecular formula $\{Gd_3^{3+}\}[Ga_2^{3+}](Ga_3^{3+}O_{12}^{2-})$ and crystallizes in a centrosymmetric space group, determined to be cubic $Ia\bar{3}d$[9] (or trigonal $R\bar{3}$ according to Ref. [10]). The Gd and Ga ions have specific site symmetry that is related to its oxygen coordinations, namely dodecahedral, octahedral and tetrahedral, respectively. Thus the site symmetry is lower than the symmetry of the crystal.

Small amounts of calcium oxide are usually added to the melt during crystal growth in order to avoid screwed growth of rare-earth GGG crystals. This helps in growing large single crys-

#8649 - $15.00 USD Received 1 September 2005; revised 9 January 2006; accepted 14 January 2006

tals for high-power laser applications. However, doping with small amounts of calcium results also in degradation of laser performance because of optical loss by irradiation induced color centers [11]. The formation of such color centers can result in induced absorption bands in the visible and UV spectral ranges and is therefore an obstacle for applications. The strong photochromic effect [12, 13] in GGG is due to its richness with color centers as a consequence of its non-stoichiometry caused by impurities or dopants. Antisite defects are formed through the replacement of the excess Gd to the octahedral Ga positions. Deficiency of gallium oxide [14] produces also vacancies of gallium (V_{Ga}) and oxygen (V_O). Exposing the crystal to an ionizing radiation generates charge carriers that can be trapped at these vacancies thus creating additional defects. Any photochromic effect is related to an induced refractive-index change through the Kramers-Kronig relation. Therefore GGG is a possible candidate for a photorefractive material suitable for information storage, provided that induced refractive index changes are high enough.

The photorefractive effect in most of the standard photorefractive materials is due to the linear electro-optic effect [15]. However, light-induced refractive-index changes were also found in centrosymmetric crystals[16, 17, 18, 19], although all odd-rank tensor elements vanish by symmetry consideration. The origin of the photorefractive effect in centrosymmetric crystals therefore is far from being understood. Usually, the effect is explained on the basis of particular properties of the involved material: it can be attributed to the quadratic electro-optic effect [20], optical excitation of infinitely long-lived metastable electronic states [18, 19], and always by photochromic behavior via Kramers-Kronig relations [17]. The photorefractive effect in centrosymmetric materials may require application of an external electric field [21] or cooling of the material to temperatures lower than 200 K [22, 23].

The aim of this Letter is to demonstrate, to investigate, and to characterize the photochromic and the photorefractive properties of GGG:Ca at room temperature by means of holographic techniques.

2. Experiment

GGG single crystals were grown by the Czochralski method. The samples are plane-parallel plates with dimensions ($10 \times 10 \times 5$ mm^3). The large faces are perpendicular to the [111] direction. Absorption spectra of the samples were collected using a Cary 500 spectrometer. The samples were irradiated using various UV ($\lambda = 351, 364$ nm) and visible lines ($\lambda = 458 \ldots 514$ nm) of an argon-ion laser or a diode-pumped solid state laser ($\lambda = 405$ nm).

Prior to any holographic measurement, the sample was heated up to 400 $^\circ$ Celsius for two hours and then cooled down to room temperature again. This procedure will be simply called 'heat treatment' in what follows. After that, the sample was irradiated with UV ($\lambda = 364$ nm) light until the transmitted intensity did not change any more. Holographic gratings were recorded by a standard two-wave mixing setup, using one of the visible lines of an argon-ion laser. Two plane waves with a beam diameter of 4 mm and equal intensities, i.e., modulation depth $m = 1$, between 10 - 30 mW/cm^2 and parallel polarization states were employed as recording beams under a crossing angle of $2\Theta = 27^\circ$(outside the medium). The resulting grating spacing thus was either 981 nm (λ_w=458 nm) or 1.1 μm (λ_w=514 nm). During recording, the diffraction efficiency $\eta = I_d/(I_d + I_f)$ is measured as a function of time by blocking one of the beams for a short time. Here, $I_{d,f}$ denote the diffracted and forward diffracted intensities, respectively. Note, that we use the definition of a *relative diffraction efficiency*, i.e., correcting for the mean absorption. The angular dependence of the diffraction efficiency is measured at the end of recording, typically after an exposure of 10-12 Ws/cm^2, using a read-out intensity that is two orders of magnitude lower than that for recording. For this type of experiment the crystal was mounted on a computer-controlled rotation stage with an angular accuracy of $10^{-3\circ}$.

#8649 - $15.00 USD Received 1 September 2005; revised 9 January 2006; accepted 14 January 2006

In addition beam-coupling experiments were performed (at the recording angle) to obtain the complete information on the physical parameters: the amplitudes of the refractive index (n_1) and the absorption (α_1) grating, the phase shift $\Delta\varphi$ between those gratings, and the phase Φ between the interference pattern and the refractive-index pattern. For this experiment the crystal was mounted on a piezoelectric translation-stage and moved in parallel to the grating vector. The intensities $I_{C1,C2}$ of the coupled beams were monitored by Si-photodiodes. A schematic of the experimental setup is shown in Fig. 1. All holographic and spectroscopic measurements were performed at room temperature.

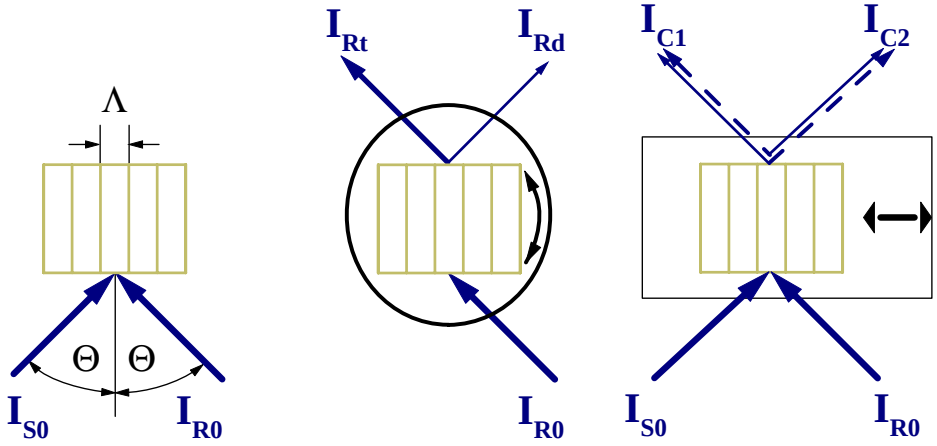

Fig. 1. Schematic of the experimental setups for recording gratings, performing rocking curves and beam-coupling experiments.

3. Experimental results

The typical absorption spectra of as-grown pure and calcium doped GGG at room temperature are shown in Fig. 2. Sharp absorption lines are observed in both, pure and doped samples. The doped sample exhibits three additional broad bands in comparison to that of the nominally pure sample: two strong overlapping bands around 340 nm (B2 band) and 250 nm (B1 band) and another weak broad band around 425 nm (B3 band) as shown in the inset of Fig. 2 in accordance with previous work[14, 24].

Induced absorption changes of a GGG:Ca single crystal due to irradiation with UV, visible light or a heat treatment are presented in Fig. 3. The room-temperature spectrum of the heat-treated sample (heating for 2 hours at 400°) is taken as the reference against which absorption changes are detected. It is evident, that UV illumination increases the bands B1 and B3, and decreases band B2. The strongest induced absorption occurs at band B3. The latter is responsible for a dark brownish color of the sample and thus we call such a state the 'colored state'. We emphasize, that the identical stationary colored state is approached upon prolonged UV irradiation, regardless of the previous treatment of the crystal. For holographic experiments to be discussed below, we illuminate the sample with UV light until a steady colored state is obtained. Annealing at elevated temperature strongly decreases band B3, so that the crystal becomes transparent again. Therefore, this final state is called the fully 'bleached state' which can also be reached irrespective of its treatment history.

As a first step in holographic measurements, we recorded an elementary holographic grating. In Fig. 4 the dependence of the diffraction efficiency on exposure $Q = I_0 t$ with $\lambda_w = \lambda_r$ = 458

#8649 - $15.00 USD Received 1 September 2005; revised 9 January 2006; accepted 14 January 2006

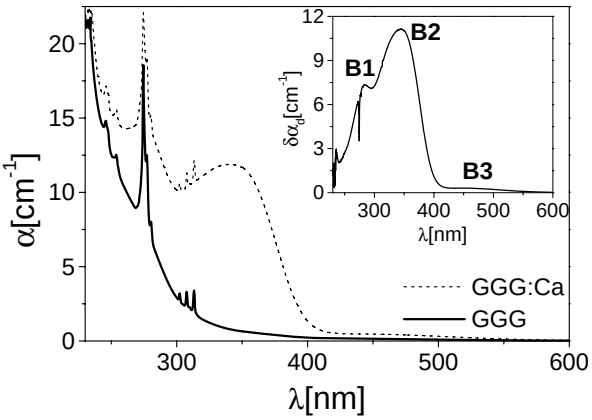

Fig. 2. Absorption spectra of as-grown pure and calcium doped single crystals of GGG at room temperature. Inset: difference $\delta\alpha_d = \alpha_{doped} - \alpha_{pure}$ of the absorption coefficient between the doped and the pure GGG sample as a function of wavelength.

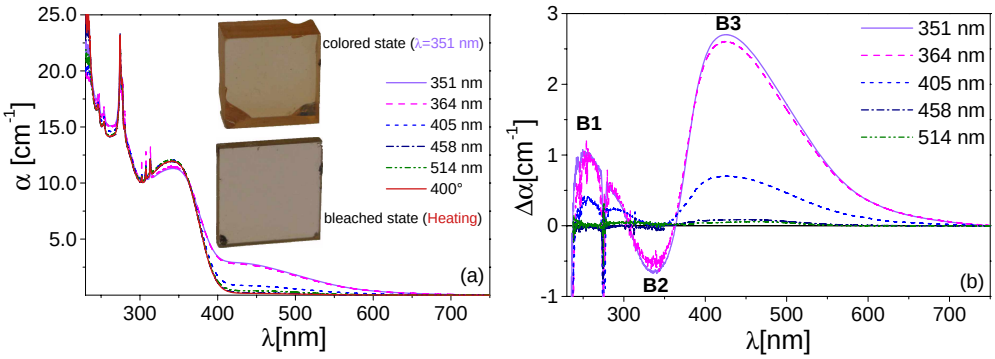

Fig. 3. Spectral dependence of the absorption coefficient of a GGG:Ca crystal illuminated with UV, visible light and after a heat treatment (a). The inset shows photographs of the sample in the bleached and the colored state, respectively. The absorption difference spectra (b) are obtained by subtraction of the spectrum for the heat-treated reference sample.

or 514 nm, I_0=11.1 and 20.3 mW/cm^2, respectively, is depicted. The subscripts *w* and *r* refer to writing and read-out, respectively. As shown in Fig. 4 the diffraction efficiency increases, passes a maximum and slightly decreases for all recording wavelengths. This resembles the behavior of recently described similar systems[25]. Gratings could be recorded at all available wavelengths in the visible range obtained from Ar-ion laser.

After recording of an elementary grating for an exposure of about 12 Ws/cm^2, the angular dependence of the diffraction efficiency was measured. Read-out was performed at the recording wavelength and polarization state, but the intensity was decreased to typically 10^{-2} of the recording intensity. Figure 5 shows the diffraction efficiency as a function of the deviation from the recording angle for each of the recording beams (S- or R-beam), where alternately the R- or S-beam is blocked. Figure 5 shows at least three distinct interesting features: (1) The width of the rocking curves is extremely small and therefore the angular sensitivity high; (2) The maximum diffraction efficiencies for the R- and S-beam differ considerably. Their ratio η_R/η_S at

#8649 - $15.00 USD Received 1 September 2005; revised 9 January 2006; accepted 14 January 2006

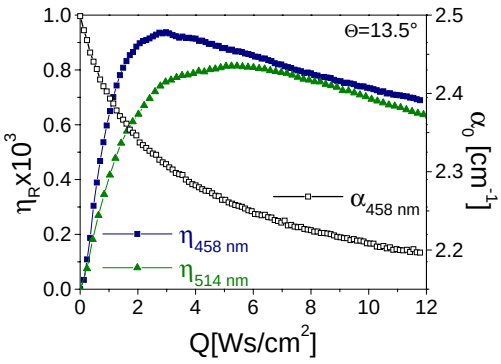

Fig. 4. Kinetics of the diffraction efficiency η_R of the R-beam during recording an elementary grating at room temperature for two different wavelengths λ_w=458 and 514 nm (left scale). The light-induced change of the mean absorption coefficient α_0 is also shown (right scale).

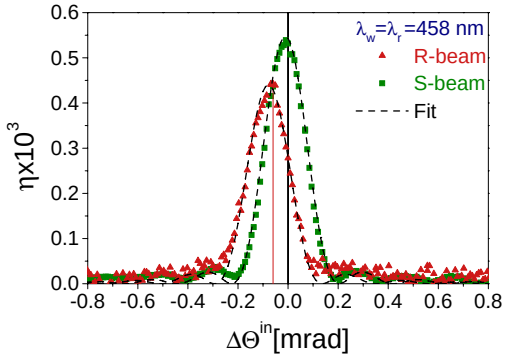

Fig. 5. Angular dependence of the $\pm 1^{st}$ order diffraction efficiency $\eta_{R,S}$ around the Bragg incidence. The grating was recorded and read out at $\lambda_w = \lambda_r = 458$ nm.

the recording angle ($\Delta\Theta = 0$) is about 0.78; (3) The position of the maximum occurs slightly outside the recording angle, i.e., the Bragg angle, for the R-beam. The second observation can be explained by mixed phase and amplitude gratings as will be discussed below.

In order to further explore the basis for the photorefractive and photochromic effect in GGG, we conducted beam coupling experiments. This type of experiments allows to evaluate the contributions of the refractive-index and absorption modulation (n_1, α_1) to the grating, a possible phase-difference $\Delta\varphi$ between them, and the phase-shift Φ between the incoming interference pattern and the grating. In our setup we simply translated the grating along its grating vector with a speed that is faster than the holographic response. The intensities $I_{C1} = |A_{Rf} + A_{Sd}|^2$ and $I_{C2} = |A_{Rd} + A_{Sf}|^2$ of the coupled beams were monitored as a function of the translation. Here, $A_{(R,S)(d,f)}$ denote the amplitudes of the diffracted and forward-diffracted R- and S-beams. The sinusoidal variation of the intensities is shown in Fig. 6.

#8649 - $15.00 USD Received 1 September 2005; revised 9 January 2006; accepted 14 January 2006

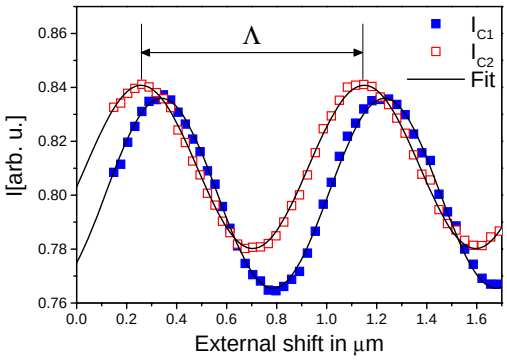

Fig. 6. Beam coupling analysis with an external displacement of the recorded elementary hologram along its grating vector. $\lambda_w = \lambda_r = 458$ nm. The grating spacing Λ is indicated. Note, that the intensities of the coupled beams are *dephased*.

4. Discussion

4.1. Spectroscopic results

Let us start the discussion with the obtained spectroscopic results and possible candidates for photorefractive centers. The well separated sharp absorption lines observed in both spectra as shown in Fig. 2 correspond to intra-center transitions of f-electrons in the Gd^{3+} ion [26].

As shown in the inset of Fig. 2 doping GGG with calcium creates three additional bands B1, B2 and B3. Moreover, illumination with UV or visible light or a heat treatment changes the density of states within these bands. This means that the centers that produce these bands are also responsible for the observed photosensitive effects. Considering the relative strength of these bands, one can see according to Fig. 3, that the major changes occur at band B3. From previous work it is known that the bands B1, B2 and B3 originate from intrinsic point defects and charge compensation which produce complex color centers (CCC) and F-centers [27, 24, 28, 14]. The calcium ion itself does not induce absorption bands, but its addition results in a charge imbalance. It is proposed that oxygen vacancies V_O or V_O associated with Ca^{2+} impurities are responsible for getting overall charge neutrality[24]. Thus a variety of intrinsic defects may be created upon doping with calcium: an oxygen vacancy V_O trapping an electron (F^+ color center) or two electrons (F color center), or the complex color centers $[Ca^{2+}F^+]$. The consequence of doping with calcium can be seen in the inset of Fig. 2. The strong band around B2 is supposed to be due the CCC [28] and the broad weak band around B3 corresponds to F-type centers [13]. Band B1 is suggested to be due to the presence of cation and anion vacancies including complexes $[V_{Ga}V_O]^-$ [14].

The defects we are particularly interested in are those, that are capable of capturing the generated charge carriers due to illumination such as V_O, V_{Ga} and V_{Gd} [13]. In a highly doped GGG the CCC play a dominant role in the radiation recharging processes [14]. CCC are ionized by UV and this leads to a decrease of the absorption band B2. Some of the released electrons from excited CCC can be trapped by V_O defects giving rise to F-centers that absorb in the spectral region around 430 nm (B3)[12, 14]. The ionized CCC, $[Ca^{2+}V_O]^+$, has an absorption band around 270 nm (B1) [28]. This is revealed from the induced absorption bands that are due to UV illumination and is depicted in Fig. 3(b).

If the crystal is heated or illuminated with visible light, electrons are released from F-centers to the conduction band that are subsequently trapped by ionized CCC, giving the original charge

#8649 - $15.00 USD Received 1 September 2005; revised 9 January 2006; accepted 14 January 2006

states of defects which lead to the bleached state[28], cf. Fig. 3(b). Thus the above mentioned generated charge transfer processes between CCC and F-centers are responsible for the photochromic phenomena in GGG.

Now we would expect that the local change of charge carriers between color centers is also responsible for a modulation of the refractive index via the Kramers-Kronig relationships. However, this implies that absorption and refractive-index gratings are *in phase* ($\Delta\varphi = 0$). Moreover, as the charge transfer processes occur at a certain site, the photosensitive effects must be strictly local, i.e., that the light-interference pattern is in phase with the grating ($\Phi = 0$). However, these expectations are in contradiction to our experimental results obtained by holography as discussed below.

4.2. Holographic results

The grating has rise times of about 53 and 42 sec for λ_w =514 and 458 nm, respectively, at the used low recording intensities. A fit according to the kinetics of a two-states model did not yield satisfactory results[25], a hint that unlike terbium gallium garnet GGG:Ca is not an optical two-states system. Next, the peculiarities of the rocking-curve (Fig. 5) will be discussed. The high angular sensitivity is due to the large thickness of the GGG crystal. Estimating the grating thickness from the position of two neighbouring minima of the rocking curve far outside the Bragg maximum, we find a value of 5 mm, i.e., the grating extends over the whole thickness of the sample.

The difference between the diffraction efficiencies η_R and η_S measured near opposite Bragg-angles can be attributed to the Borrmann-effect. In common photosensitive materials either the contribution of the phase or the amplitude grating is negligible. Even if they are of the same order of magnitude but *in phase*, the diffraction efficiency simply is made up of two separate terms. One is due to the phase grating and the other to the absorption grating. A Borrmann-effect only occurs, if a phase-grating and an amplitude-grating co-exist that are *dephased*. Then the angular dependence of the diffraction efficiencies is not a simple superposition of two contributions any more. This case was analytically treated for the first time by Guibelalde[29]. We adopt a different notation here, that emphasizes the basic structure

$$\eta_{R,S} = \frac{(n_1\pi/\lambda)^2 + (\alpha_1/2)^2 \pm n_1\pi\alpha_1/\lambda \sin(\Delta\varphi)}{X^2 + Y^2} \left[\sin^2(\mathrm{Xd}) + \sinh^2(\mathrm{Yd})\right]. \qquad (1)$$

Here, $X = X(n_1, \alpha_1, \Delta\varphi, \Delta\theta), Y \in \mathbb{C}$ are functions of the corresponding parameters, including the angular deviation $\Delta\theta$ from the Bragg-angle. The $\pm$-signs are valid for the R- and S-beam, respectively. From Eq. 1 the ratio η_R/η_S at the Bragg angle amounts to

$$\frac{\eta_R}{\eta_S} = \frac{(n_1\pi/\lambda)^2 + (\alpha_1/2)^2 + n_1\pi\alpha_1/\lambda \sin(\Delta\varphi)}{(n_1\pi/\lambda)^2 + (\alpha_1/2)^2 - n_1\pi\alpha_1/\lambda \sin(\Delta\varphi)}. \qquad (2)$$

Therefore, a Borrmann effect cannot occur in the case of $\Delta\varphi \equiv 0$ and hence, our experimental results prove that in GGG mixed phase and absorption-gratings were generated, that are out of phase. Fitting Eq. 1 to the rocking-curves is possible, but the determination of the parameters is not unique. Only the thickness d can be extracted. We note, that from the rocking-curve we obtain for the ratio *at the recording geometry* $\eta_R/\eta_S = 0.526$.

A puzzling feature of the rocking-curves shown in Fig. 5 is, that the maximum diffraction efficiency does not occur at the recording angle for the R-beam, but at $\Delta\theta_R = -0.06$ mrad. Though this shift is very small, it is distinctive and reproducible. It would be straightforward to attribute this shift to transient effects, that originate from a dissimilarity in the intensities of the recording beams in local response media[30]. In this case, the recording itself breaks the symmetry and in the steady state the gratings are slanted. On one hand, this is supported by

#8649 - $15.00 USD Received 1 September 2005; revised 9 January 2006; accepted 14 January 2006

two measurements where $I_R \lesssim I_S$ or $I_R \gtrsim I_S$. Here, we found that the sign of the shift depends on the sign of $1 - I_R/I_S$ for the recording beams. However, in the case of a slanted grating we would expect that η_S shows a similar behavior, i.e., its maximum is shifted to the same angular deviation, which is not the case. Next, we assumed that it might simply originate from the fact, that the angular sensitivity of the crystal is too high for the accuracy of the rotation stage ($10^{-3\circ}$). Experiments with a thinner sample ($d = 1.6$ mm) were conducted that yielded the same result: A shift of the diffraction efficiency from its recording angle, which is different for the R- and S-beam. Therefore, the reason for the shift of the maximum diffraction efficiency in its angular position remains unclear.

Beam coupling experiments in the *recording geometry* were conducted, that enable us to determine the characteristic parameters $n_1, \alpha_1, \Delta\varphi$ and in addition the relative phase Φ between the light interference pattern and the (refractive-index) grating. The intensities of the coupled beams I_{C1} and I_{C2} , i.e., the transmitted R-beam and the diffracted S-beam and vice versa, are monitored as a function of the externally applied phase-shift. Then the parameters can be evaluated by a Fourier analysis of the experimental data [31]. However, due to the angular deviation from the recording geometry, we have to redefine the parameters $a_{R,S}, b_{R,S}, c_{R,S}$ from Ref. [31]. This is necessary to correctly account for an additional phase-shift originating from the Off-Bragg geometry. Hence, in the notation of Ref. [31] with Φ instead of $\phi_{p,0}$, and assuming $A_{R,S} \in \mathbb{R}$ without loss of generality

$$a_R := A_R^2 \hat{R}_+ \hat{R}_+^* + A_S^2 \hat{S}_- \hat{S}_-^* \qquad a_S := A_S^2 \hat{R}_+ \hat{R}_+^* + A_R^2 \hat{S}_- \hat{S}_-^* \tag{3}$$

$$b_R := 2A_R A_S \Re\{\hat{R}_+^* \hat{S}_- e^{i\Phi}\} \qquad b_S := 2A_R A_S \Re\{\hat{R}_- \hat{S}_+^* e^{i\Phi}\} \tag{4}$$

$$c_R := 2A_R A_S \Re\{\hat{R}_+^* \hat{S}_- i e^{i\Phi}\} \qquad c_S := 2A_R A_S \Re\{\hat{R}_- \hat{S}_+^* i e^{i\Phi}\}. \tag{5}$$

Note, that $\hat{R}_\pm, \hat{S}_\pm$ are functions of $n_1, \alpha_1, \pm\Delta\varphi, \pm\Delta\theta$ with the abbreviation $\hat{R}_\pm = \hat{R}(n_1, \alpha_1, \pm\Delta\varphi, \pm\Delta\theta)$. Taking the grating thickness ($d = 5$ mm) as a fixed parameter in fitting the beam coupling measurements, we obtained the following values: $n_1 = 1.4 \times 10^{-7}, \alpha_1 = 8.8/\mathrm{m}, \Delta\varphi = -48^\circ, \Phi = 68^\circ$. In addition the amplitudes of the beams inside the medium are evaluated as $A_S = 0.9, A_R = 0.894$, so that the modulation depth is nearly unity. The ratio of the diffraction efficiencies at the *recording geometry* is 0.526, which is exactly the same as obtained from the rocking-curve.

Two strange peculiarities are obvious: $\Delta\varphi \neq 0$. Usually it is argued, that Kramers-Kronig relations provide a refractive-index change in photochromic materials. However, in this case their must not be any phase-shift between the amplitude grating and the phase grating. This is similar to recently obtained results in bleached silver halide materials[32]. In addition also a dephasing between the interference pattern and the refractive-index grating occurs. Therefore, non-locality of the photorefractive effect is demonstrated. This enables the process of holographic amplification via two-wave mixing.

Even if we assume a certain error in evaluating our data, these results indicate, that the phase-shifts Φ and $\Delta\varphi$ are definitely different from 0 or $\pi/2$ as usually expected. Moreover, the shift of the angular position of the maximum in the diffraction efficiency violates the assumption, that GGG has a center of inversion. This is equivalent to saying that by illumination with a sinusoidal interference pattern the *centrosymmetric structure is broken* in our crystal. To reveal the origin for this phenomenon needs further investigations.

In summary, in this work we report the presence of a photorefractive and photochromic effect a GGG crystal doped with calcium. By employing a holographic two-wave mixing setup we recorded mixed phase-amplitude gratings at room temperature. The presence of the Borrmann effect, an angular shift of the maximum diffraction efficiency in rocking curves and a beam-coupling analysis revealed, that the gratings are out of phase and thus a light-induced

#8649 - $15.00 USD Received 1 September 2005; revised 9 January 2006; accepted 14 January 2006

symmetry break has occurred. We agree, that the facts presented here are counter-intuitive for a centrosymmetric crystal. The physical origin for this symmetry break is not yet known.

Although the diffraction efficiency of GGG:Ca is low, it is interesting to further investigate the light-induced properties for the following reasons: the photorefractive effect even persists at room temperature, the crystal is available in an excellent optical quality and large size, and the tempting perspective to realize any optical element for optical data storage and processing with a single material class (garnets).

Acknowledgment

We acknowledge continuous support by E. Tillmanns. This work was financially supported by the Austrian Science Fund (P-15642), the Research and Technology Innovation Fund and the Bundesministerium für Auswärtige Angelegenheiten in the frame of the Hungarian-Austrian scientific and technological cooperation ÖAD- WTZ A-8/2003.

#8649 - $15.00 USD Received 1 September 2005; revised 9 January 2006; accepted 14 January 2006